Electronic Supplementary Material (ESI) for Journal of Materials Chemistry A.

Supporting Information

Unravelling Binder Chemistry in Sodium/Potassium Ion Batteries for Superior Electrochemical Performances

Chunting Wang,[a] Long Su,[a] Nana Wang,[b] Dan Lv,[a] Dongdong Wang,[a] Jian Yang,*[a] and Yitai Qian[ac]

a. C. Wang, L. Su, D. Lv, D. Wang, Prof. J. Yang, Prof. Y. Qian
Key Laboratory of Colloid and Interface Chemistry, Ministry of Education, School of Chemistry and Chemical Engineering
Shandong University
Jinan 250100, P. R. China
E-mail: yangjian@sdu.edu.cn

b. Institute for Superconducting and Electronic Materials University of Wollongong Innovation Campus
Innovation Campus, Squires Way, Wollongong
New South Wales 2500, Australia

c. Hefei National Laboratory for Physical Science at Microscale
Department of Chemistry
University of Science and Technology of China
Hefei 230026, P. R. China

Table S1. Initial Coulombic Efficiency (iCE) of TiO_2-based anodes.

Ref.	iCE	Electrolyte
1	26.0%	EC: DEC (1:1 by weight) with 5wt % FEC
2	46.0%	EC: DEC (1:1 by weight) with 5wt % FEC
3	44.5%	EC: DMC (1:1 by volume) with 2 % FEC
4	58.2%	EC: DMC (1:1 by volume)
5	58.8%	EC: DMC (1:1 by volume) with 5wt % FEC
6	76.0%	Diglyme
7	45.2%	Diglyme with 5% FEC
8	80.0%	DME
9	54.3%	Diglyme
10	68.6%	Diglyme
11	76.0%	Diglyme

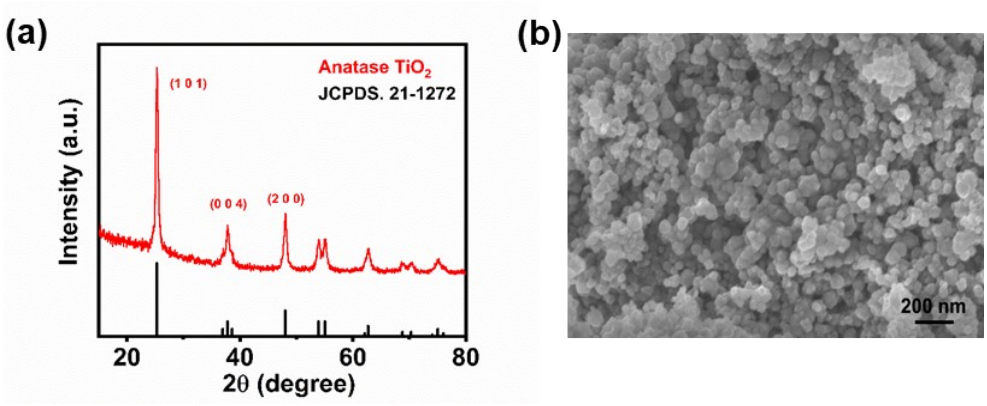

Fig. S1 (a) XRD pattern and (b) SEM image of commercial TiO_2 nanoparticles.

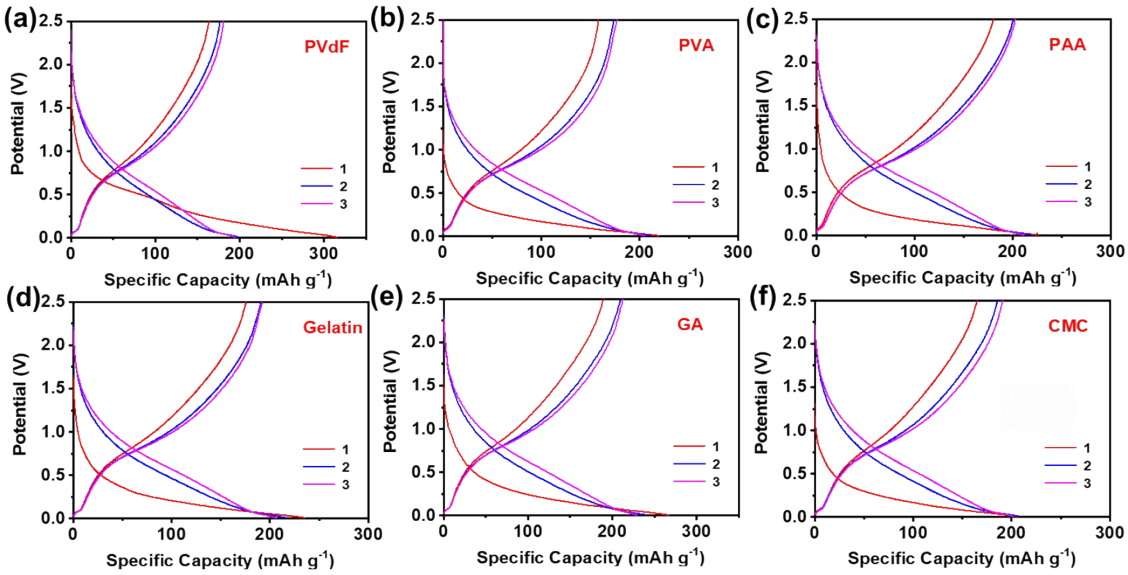

Fig. S2 Discharge/charge voltage profiles of the electrodes using different binders. (a) PVdF, (b) PVA, (c) PAA, (d) Gelatin, (e) GA, and (f) CMC.

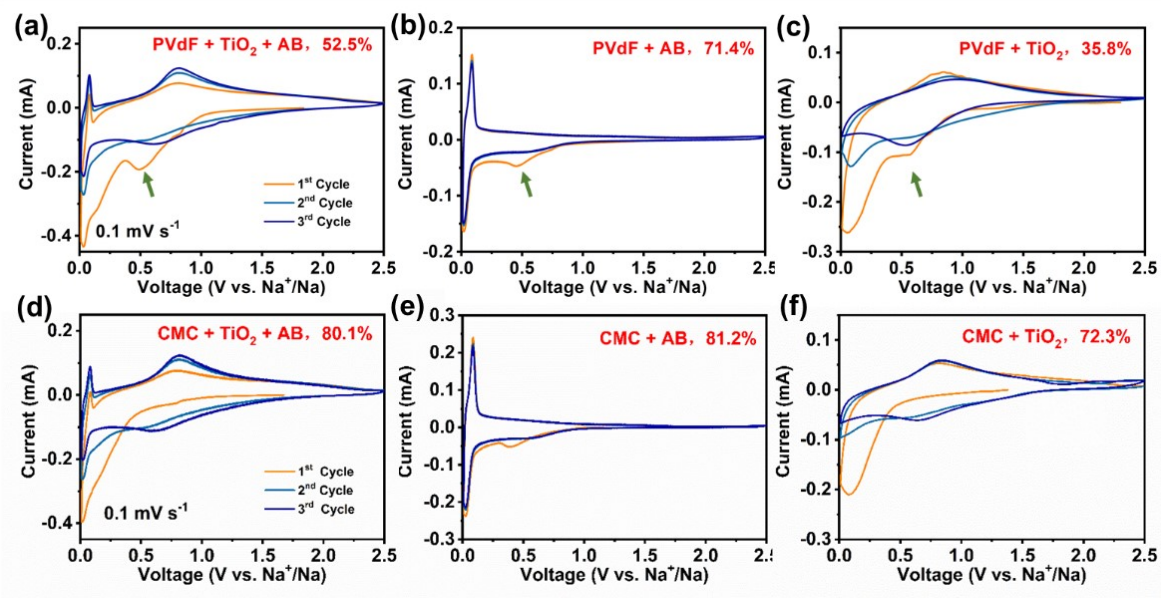

Fig. S3 CV curves of the electrodes using different recipes. (a) PVdF+AB+TiO_2, (b) PVdF+AB, (c) PVdF+TiO_2, (d) CMC+ AB+TiO_2, (e) CMC+AB, and (f) CMC+TiO_2.

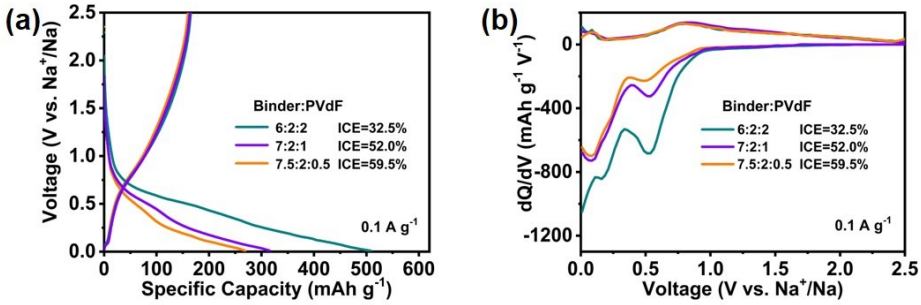

Fig. S4 (a) Discharge/charge voltage profiles and (b) dQ/dV curves of the electrodes using different contents of PVdF in the electrode. Here, 7:2:1 indicates that the electrode contains 70 wt% TiO_2, 20 wt% AB and 10 wt% PVdF.

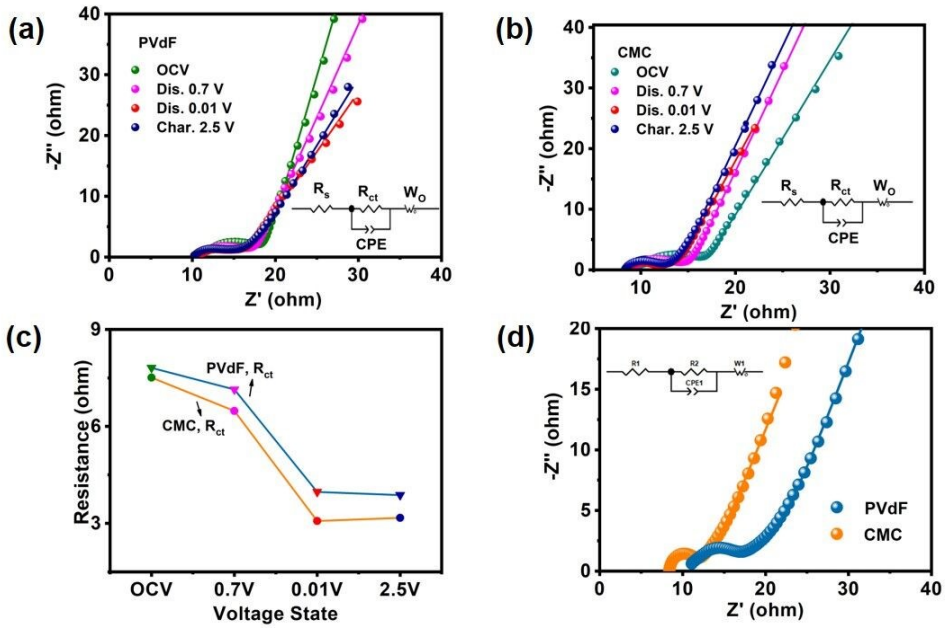

Fig. S5 (a) EIS spectra of the electrodes at different states of discharge in the first cycle. (b) EIS spectra of the electrodes at different states of charge in the first cycle. (c) Comparison of R_{ct} for the electrodes using different binders. (d) EIS spectra of the electrodes using different binders after 10 cycles.

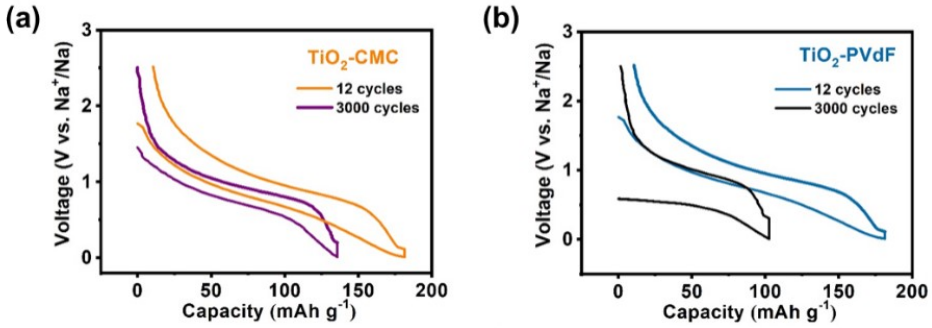

Fig. S6 Charge and discharge profiles of the electrodes with (a) CMC or (b) PVdF as the binder after 12 cycles and 3000 cycles.

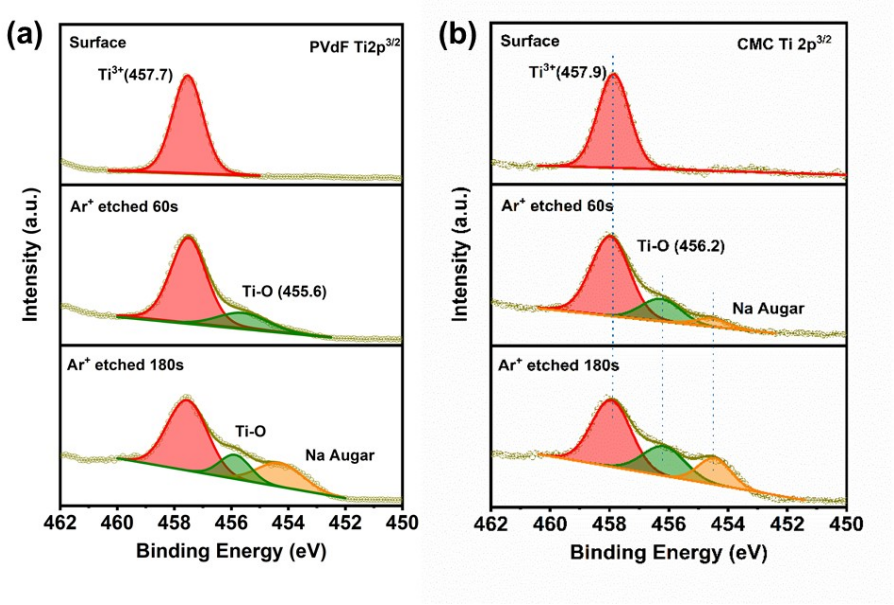

Fig. S7 High-resolution Ti $2p^{3/2}$ spectra of the electrodes using (a) PVdF or (b) CMC as binder after the first discharge to 0.01 V.

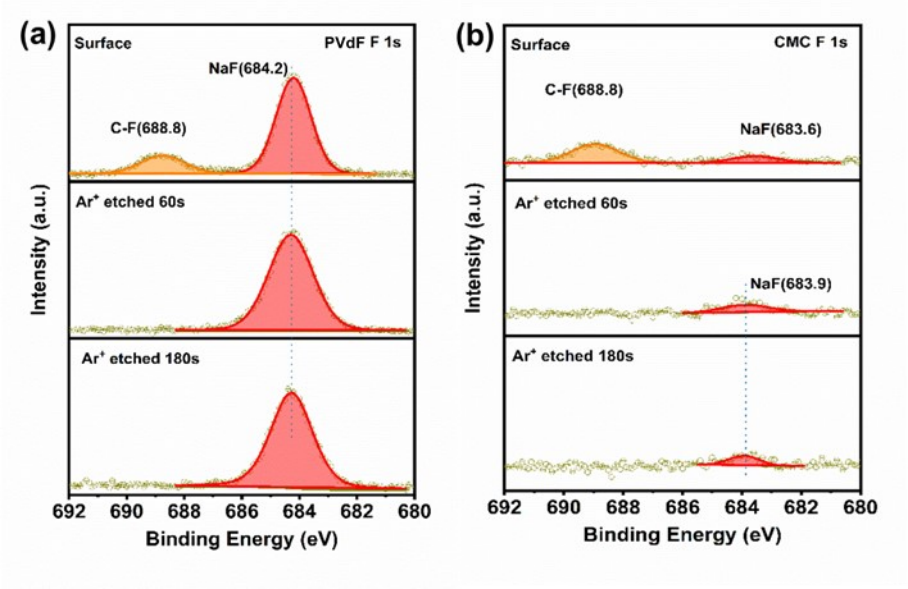

Fig. S8 High-resolution F*1s* spectra of the electrodes using (a) PVdF or (b) CMC as binder after the first discharge to 0.01 V.

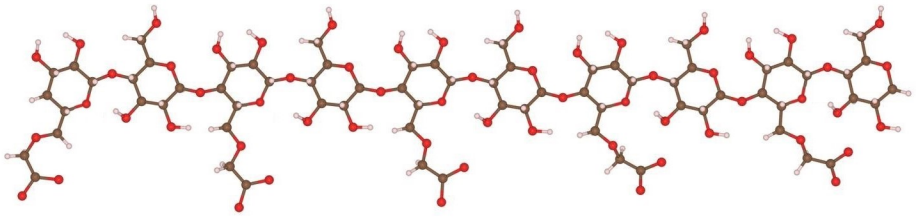

Fig. S9 Structure diagram of CMC used for DFT calculation.

Fig. S10 Structure diagram of PVdF used for DFT calculation.

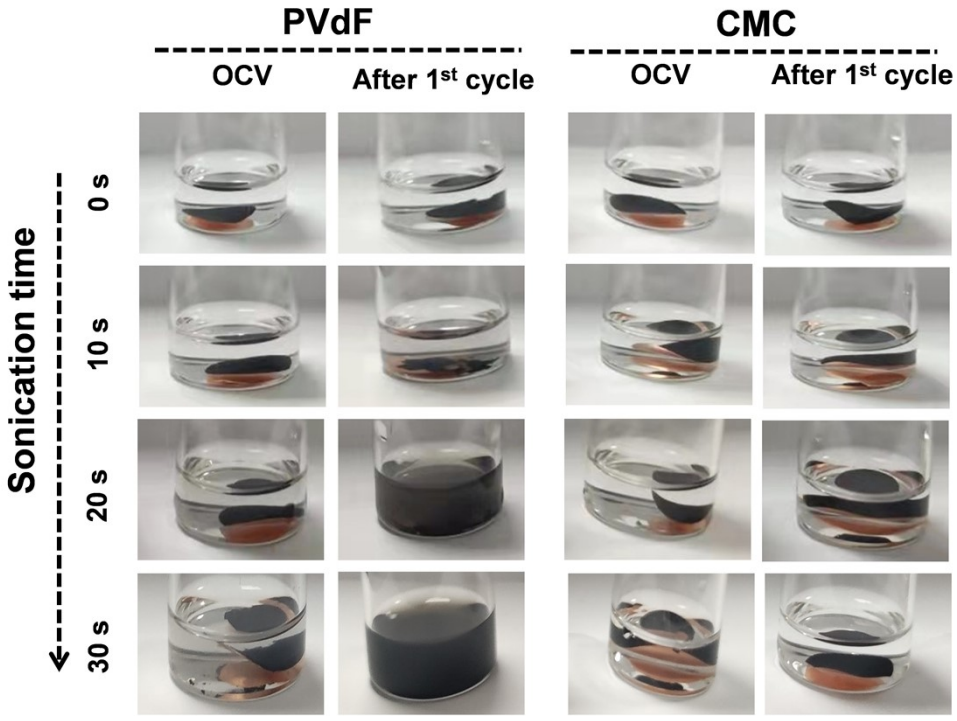

Fig. S11 Real images of the electrodes using different binders after ultrasonication.

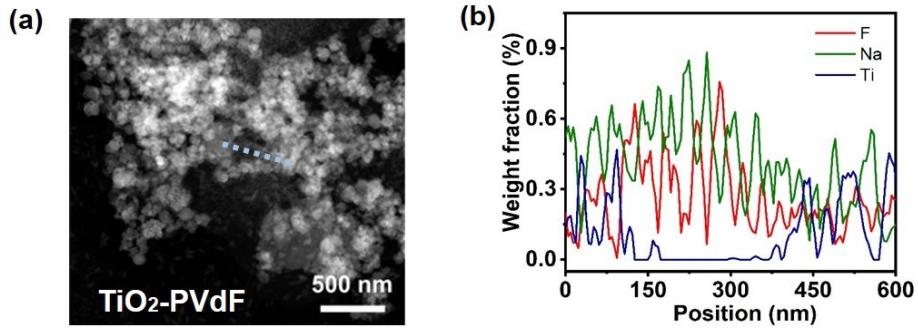

Fig. S12 (a) HAADF-STEM image, and the (b) line scanning profiles of Ti, Na, F along the dash line in the electrode after the first cycle using PVdF as binder.

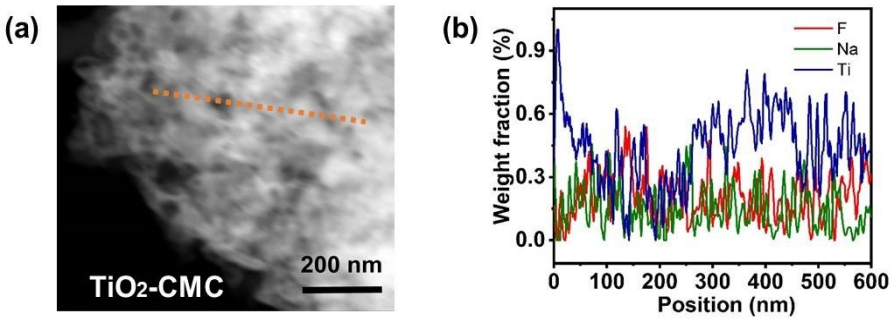

Fig. S13 (a) HAADF-STEM image, and the (b) line scanning profiles of Ti, Na, F along the dash line in the electrode after the first cycle using CMC as binder.

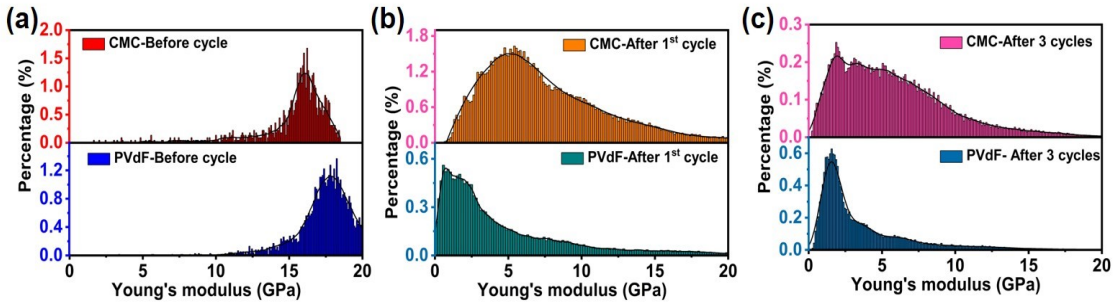

Fig. S14 Young's modulus distribution of the electrodes using CMC or PVdF as the binder. (a) Before cycle, (b) after the first cycle, (c) after 3 cycles.

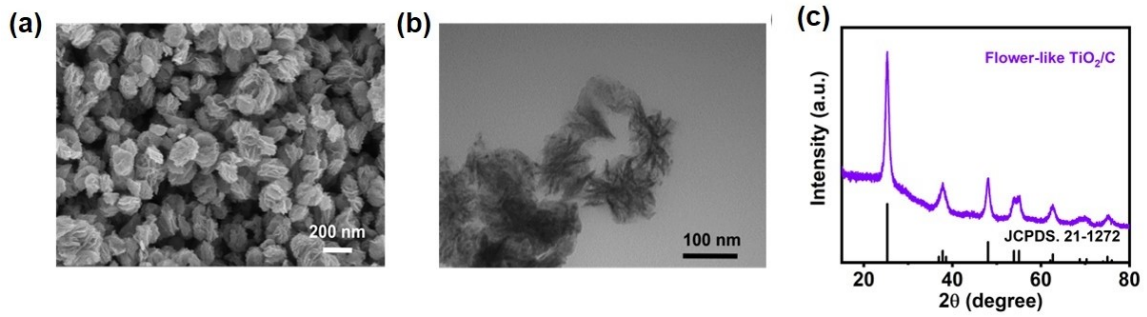

Fig. S15 (a) SEM image, (b) TEM image and (c) XRD pattern of flower-like TiO_2/C.

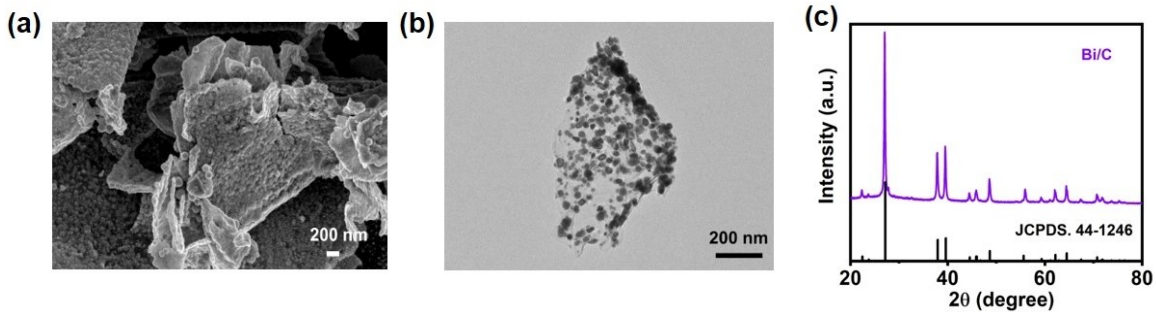

Fig. S16 (a) SEM image, (b) TEM image and (c) XRD pattern of Bi/C nanoparticles.

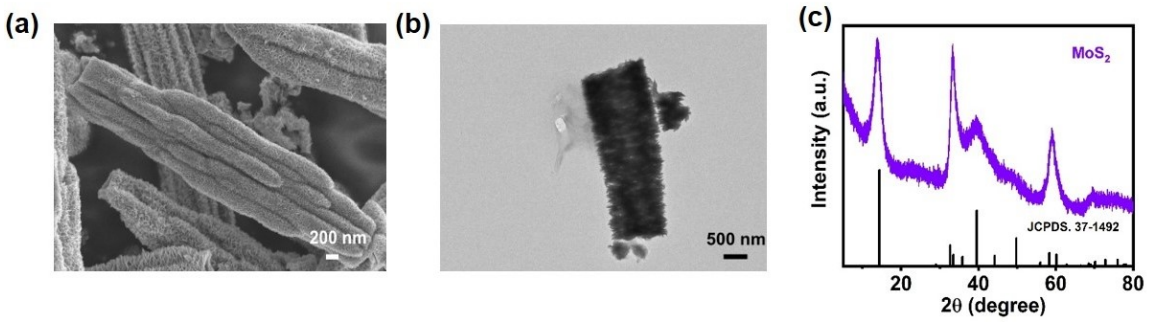

Fig. S17 (a) SEM image, (b) TEM image and (c) XRD pattern of MoS_2 nanoparticles.

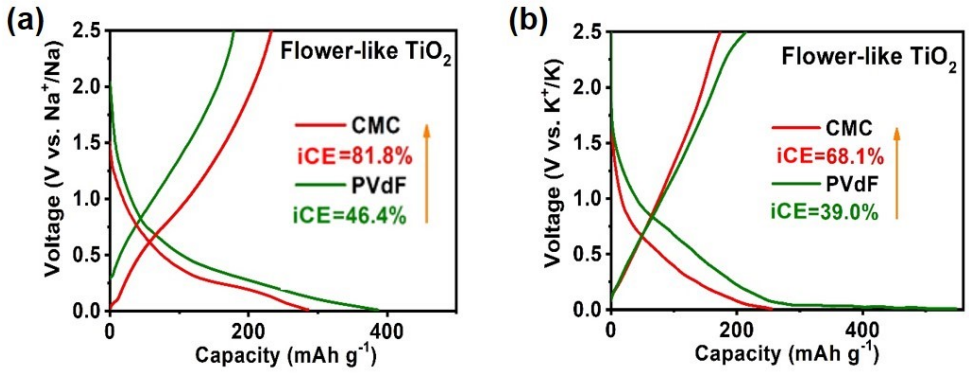

Fig. S18 Advantages of CMC over PVdF as the binder using flower-like TiO_2/C as the anode materials in SIBs.

References

1 L. Huang, L. Zeng, J. Zhu, L. Sun, L. Yao, L. Deng, P. Zhang, *J. Power Sources*, 2021, **493**, 229678.

2 Y. Tian, J. Julio Gutiérrez Moreno, Z. Lu, L. Li, M. Hu, D. Liu, Z. Jian, X. Cai, *Chem. Eng. J.*, 2021, **407**, 127198.

3 R. Luo, Y. Ma, W. Qu, J. Qian, L. Li, F. Wu, R. Chen, *ACS Appl. Mater. Interfaces*, 2020, **12**, 23939-23950.

4 L. Fu, Q. Wang, H. He, Y. Tang, H. Wang, H. Xie, *J. Power Sources*, 2021, **489**, 229516.

5 J. Ma, M. Xing, L. Yin, K. San Hui, K. N. Hui, *Appl. Surf. Sci.*, 2021, **536**, 147735.

6 M. Ni, D. Sun, X. Zhu, Q. Xia, Y. Zhao, L. Xue, J. Wu, C. Qiu, Q. Guo, Z. Shi, X. Liu, G. Wang, H. Xia, *Small*, 2020, **16**, 2006366.

7 M. Fan, Z. Lin, P. Zhang, X. Ma, K. Wu, M. Liu, X. Xiong, *Adv. Energy Mater.*, 2021, **11**, 2003037.

8 B. Zhao, Q. Liu, Y. Chen, Q. Liu, Q. Yu, H. B. Wu, *Adv. Funct. Mater.*, 2020, **30**, 2002019.

9 Z. Liu, W. Zhang, Z. Zhou, X. Liu, H. Zhang, M. Wei, *ACS Appl. Energy Mater.*, 2020, **3**, 3619-3627.

10 K. Li, J. Zhang, D. Lin, D. W. Wang, B. Li, W. Lv, S. Sun, Y. B. He, F. Kang, Q. H. Yang, L. Zhou, T. Y. Zhang, *Nat. Commun.*, 2019, **10**, 725.

11 K. Lan, L. Liu, J. Zhang, R. Wang, L. Zu, Z. Lv, Q. Wei, D. Zhao, *J. Am. Chem. Soc.*, 2021, **143**, 14097.